STEM CELLS®

EMBRYONIC STEM CELLS/INDUCED PLURIPOTENT STEM CELLS

Undifferentiated Embryonic Cell Transcription Factor 1 Regulates ESC Chromatin Organization and Gene Expression

SUSANNE M. KOOISTRA,[a] VINCENT VAN DEN BOOM,[b] RAJKUMAR P. THUMMER,[a] FRANK JOHANNES,[c] RENÉ WARDENAAR,[c] BRUNO M. TESSON,[c] LIESBETH M. VEENHOFF,[d] FABRIZIA FUSETTI,[d] LAURA P. O'NEILL,[e] BRYAN M. TURNER,[e] GERALD DE HAAN,[b] BART J. L. EGGEN[a,f]

[a]Department of Developmental Genetics, Groningen Biomolecular Sciences and Biotechnology Institute, University of Groningen, Haren, The Netherlands; [b]Department of Cell Biology, Section Stem Cell Biology, University Medical Center Groningen, Groningen, The Netherlands; [c]Groningen Bioinformatics Centre, University of Groningen, Haren, The Netherlands; [d]Department of Biochemistry, Netherlands Proteomics Centre, University of Groningen, Groningen, The Netherlands; [e]Chromatin and Gene Expression Group, Institute of Biomedical Research, University of Birmingham Medical School, Birmingham, United Kingdom; [f]Department of Neuroscience, Section Medical Physiology, University Medical Center Groningen, Groningen, The Netherlands

Key Words. Embryonic stem cells • Epigenetics • Gene expression • Pluripotent stem cells • Self-renewal

ABSTRACT

Previous reports showed that embryonic stem (ES) cells contain hyperdynamic and globally transcribed chromatin—properties that are important for ES cell pluripotency and differentiation. Here, we demonstrate a role for undifferentiated embryonic cell transcription factor 1 (UTF1) in regulating ES cell chromatin structure. Using chromatin immunoprecipitation-on-chip analysis, we identified >1,700 UTF1 target genes that significantly overlap with previously identified Nanog, Oct4, Klf-4, c-Myc, and Rex1 targets. Gene expression profiling showed that UTF1 knock down results in increased expression of a large set of genes, including a significant number of UTF1 targets. UTF1 knock down (KD) ES cells are, irrespective of the increased expression of several self-renewal genes, Leukemia inhibitory factor (LIF) dependent. However, UTF1 KD ES cells are perturbed in their differentiation in response to dimethyl sulfoxide (DMSO) or after LIF withdrawal and display increased colony formation. UTF1 KD ES cells display extensive chromatin decondensation, reflected by a dramatic increase in nucleosome release on micrococcal nuclease (MNase) treatment and enhanced MNase sensitivity of UTF1 target genes in UTF1 KD ES cells. Summarizing, our data show that UTF1 is a key chromatin component in ES cells, preventing ES cell chromatin decondensation, and aberrant gene expression; both essential for proper initiation of lineage-specific differentiation of ES cells. STEM CELLS *2010;28:1703–1714*

Disclosure of potential conflicts of interest is found at the end of this article.

INTRODUCTION

Embryonic stem (ES) cell lineage specification requires the orchestrated activation of developmental gene expression programs. These processes are controlled by regulatory systems operating at three different hierarchical levels, that is, the spatial and temporal regulation of gene expression at the single gene level, the organization of chromatin into higher order domains, and the spatial arrangement of chromosomes in the nuclear space [1, 2].

The structure of chromatin and the transcriptional activity of the genes within that chromatin is mainly determined by post-translational modification of histones. Transcriptionally inactive heterochromatin is generally associated with trimethylation of lysine 9 of histone H3 (H3K9), H3K27, and H4K20 in combination with low levels of acetylation. Euchromatin, which is actively transcribed, is typically associated with high levels of acetylation and trimethylation of H3K4, H3K36, and H3K79 [3]. In ES cells, many developmental genes contain "bivalent" domains that carry both repressive (H3K27me3) and active (H3K4me3 or H3K9Ac) marks. These genes are postulated to be "poised" for transcriptional activation [4, 5].

It has become clear that ES cells have a chromatin structure (reviewed in [6, 7]), DNA methylation patterns [8], and nuclear organization [9, 10] that is very different from differentiated somatic cells. Chromatin in ES cells is highly

Author contributions: S.M.K.: conception and design, collection and/or assembly of data, data analysis and interpretation, manuscript writing; V.v.d.B.: conception and design, collection and/or assembly of data, data analysis and interpretation, manuscript writing; R.P.T.: collection and/or assembly of data; F.J.: data analysis and interpretation; R.W.: data analysis and interpretation; B.M.T.: data analysis and interpretation; L.M.V.: collection and/or assembly of data, data analysis and interpretation; F.F.: collection and/or assembly of data, data analysis and interpretation; L.P.O.: collection and/or assembly of data, manuscript writing; B.M.T.: manuscript writing; G.d.H.: manuscript writing; B.J.L.E.: conception and design, collection and/or assembly of data, data analysis and interpretation, manuscript writing, final approval of manuscript. S.M.K. and V.v.d.B. contributed equally to this article.

Correspondence: Bart J. L. Eggen, Ph.D. Telephone: +31-50-3632136; Fax: +31-50-3632751; e-mail: b.j.l.eggen@med.umcg.nl Received April 22, 2010; accepted for publication July 26, 2010; first published online in STEM CELLS *EXPRESS* August 16, 2010. 1066-5099/2009/$30.00/0 doi: 10.1002/stem.497

dynamic and a fraction of architectural chromatin proteins, including core histone proteins and heterochromatin protein 1 (HP1), is reported to be more loosely associated to the chromatin than in somatic cells [11]. The requirement of this chromatin organization for normal embryonic development is supported by numerous observations showing that interference with either histone modifying enzymes or DNA methylation results in perturbed embryonic development (reviewed in [12]).

Furthermore, it was reported that ES cells are transcriptionally hyperactive, many genes and normally silent noncoding regions are expressed in ES cells, possibly reflecting their open chromatin state [13]. Recently, Gaspar-Maia and coworkers showed that the chromatin remodeling factor Chd1 is essential for the maintenance of an open chromatin structure and pluripotency in ES cells [14]. Additionally, unlike differentiated somatic cells, ES cells are relatively unaffected in terms of self-renewal by DNA hypomethylation caused by the inactivation of the DNA methyltransferases Dnmt1 or Dnmt3a, and Dnmt3b [15–19].

It has been postulated that for ES cells to remain pluripotent, unwanted transcription of genes (transcriptional noise) should be reduced or prevented [20]. In addition to epigenetic control of transcription in ES cells, Szutorisz an coworkers demonstrated that in ES cells the proteasome targets preinitiation complexes, thus reducing transcriptional noise and preventing excessive spreading of permissive chromatin [21].

To summarize these findings, in contrast to somatic cells, ES cells contain decondensed, hyperdynamic, globally transcribed chromatin and many genes are primed to be expressed but kept in check by repressive histone modifications.

We have previously identified undifferentiated embryonic cell transcription factor 1 (UTF1) as a chromatin component in both mouse and human ES cells [22, 23]. UTF1 has core histone properties and is required for embryonic carcinoma (EC) and ES cell differentiation [22].

Recently, it was reported that the efficiency of induced pluripotent stem (iPS) cell generation was increased ~100-fold when in addition to c-Myc, Oct4, Sox-2, and Klf4, also UTF1 and small interfering RNAs against p53 were used to reprogram human fibroblasts. When UTF1 was used in combination with Oct4, Sox-2, and Klf4, replacing c-Myc, the efficiency of iPS cell generation was increased 10-fold compared with the cocktail with c-Myc. More importantly, addition of UTF1 to the cocktail greatly improved the quality of the obtained clones resulting in more ES-like iPS cells [24]. These data strongly suggest that, during reprogramming, UTF1 facilitates the formation of a chromatin structure that is important for pluripotency.

Here, we investigated the role of UTF1 in the regulation of chromatin structure and gene expression in ES and EC cells. We applied a chromatin immunoprecipitation (ChIP)-on-chip approach to identify UTF1 target genes and measured gene expression changes after UTF1 knock down in ES cells. Finally, we investigated the chromatin properties of UTF1 targets both in wild-type and UTF1 knock down (KD) ES cells.

Materials and Methods

Cell Culture

P19CL6 cells [25] were cultured in Minimal Essential Medium-α medium (Invitrogen, Breda, The Netherlands, www.invitrogen.com) supplemented with 10% fetal bovine serum (FBS) (PAA Laboratories, Colbe, Germany, www.paa.com) and 100 U/ml penicillin; 100 μg/ml streptomycin (Invitrogen). E14 IB10 ES cells were grown on gelatin-coated dishes in buffalo rat liver (BRL) cell-conditioned Dulbecco's modified Eagle's medium (DMEM) supplemented with 1,000 U/ml leukemia inhibitory factor (Millipore, Billerica, MA, www.millipore.com), nonessential amino acids (Invitrogen), and 0.1 mM 2-mercaptoethanol. Differentiation of P19CL6 cells and cell lines stably expressing UTF1 siRNA were described previously [22]. For DMSO differentiation of wt and UTF1 KD IB10 ES cells, 3.65×10^5 cells were seeded in 6-cm ø plates in DMEM (BioWhittakar, Verviers, Belgium, www.lonza.com) containing 10% fetal bovine serum (FBS) (PAA), antibiotics, and 1% DMSO (Sigma-Aldrich, Zwijndrecht, The Netherlands, www.sigmaaldrich.com). For retinoic acid (RA) differentiation, 3×10^5 cells were seeded in 0.1% gelatin coated 10-cm Petri dishes in DMEM (BioWhittakar) supplemented with 10% FBS (PAA), antibiotics, and 5 μM RA. Colony formation was assessed by seeding 250, 500, and 1,000 cells in triplicate in 10-cm gelatin-coated Petri dishes in BRL-conditioned DMEM medium containing LIF. After 8 days, cells were fixed with methanol, stained with Giemsa, and colonies counted.

Chromatin Preparation and Native Chromatin Immunoprecipitation

Chromatin preparation was performed as described [26]. Briefly, 1×10^8 cells were harvested by trypsinization, washed three times with cold PBS/5 mM sodium butyrate and resuspended in 1× Tris-buffered saline (TBS) (15 mM NaCl, 10 mM Tris-HCl, pH 7.5, 3 mM $CaCl_2$, 2 mM $MgCl_2$, 5 mM sodium butyrate and protease inhibitors) at a concentration of 2×10^7 cells/ml. An equal volume of 1× TBS/1% Tween 40 was added to the cell suspension, stirred for 1 hour on ice, followed by disruption of the cells using a Dounce all-glass homogenizer with a type A pestle. Nuclei were isolated by loading the homogenate on a discontinuous 25%–50% (w/v) sucrose gradient followed by centrifugation (3,000 rpm, 25 minutes, 4°C). The pellet was resuspended in digestion buffer (0.32 M sucrose, 50 mM Tris-HCl, pH 7.5, 4 mM $MgCl_2$, 1 mM $CaCl_2$, 5 mM sodium butyrate, and protease inhibitors). Nuclei were pelleted (2,000 rpm, 10 minutes, 4°C) and resuspended in digestion buffer at a concentration of 0.5 mg/ml (as determined by A_{260} measurement). Next, nuclei were treated with micrococcal nuclease (MNase; Sigma; 0.6 U/0.5 mg/ml nuclei) for 5 minutes at 37°C and the reaction was stopped by addition of 5 mM EDTA and samples were placed on ice for 5 minutes. Subsequently, the reactions were centrifuged (13,000 rpm, 5 minutes, 4°C), the supernatant was isolated (fraction S1), and the pellet was resuspended in lysis buffer (1 mM Tris-HCl, pH 7.4, 0.2 mM Na_2EDTA, 5 mM sodium butyrate, and 0.2 mM phenylmethylsulfonyl fluoride). These were dialyzed overnight and centrifuged (2,000 rpm, 10 minutes, 4°C) to isolate extracted chromatin (fraction S2). Fractions S1 and S2 were analyzed on an agarose gel, combined, and used for native chromatin immunoprecipitation (NChIP) analysis.

For NChIP reactions, 100 μg chromatin was incubated overnight with 50 μl of polyclonal UTF1 antibody [22] or preimmune serum as a control. Next, 100 μl 50% (w/v) protein A-Sepharose (Sigma) bead slurry was added and reactions were incubated for 3 hours at room temperature, followed by seven washes with 10 ml washing buffer (200 mM NaCl, 50 mM Tris-HCl, pH 7.5, 10 mM EDTA, and 5 mM sodium butyrate). Subsequently, beads were eluted by two consecutive 15-minute room temperature incubations with 125 μl lysis buffer containing 1% SDS and an equal volume of lysis buffer was added. DNA was isolated by two phenol/chloroform extractions and one chloroform extraction,

followed by EtOH precipitation and quantification using the Quant-iT Picogreen dsDNA Assay Kit (Invitrogen). Precipitated proteins were isolated from the organic phase from the first phenol/chloroform extraction. Five micrograms of bovine serum albumin, 1/100th volume 10 M H_2SO_4, and 12 volumes acetone were added to the phenol/chloroform phase and proteins were precipitated overnight at −20°C. After centrifugation, pellets were washed once with acidified acetone (1:6, 100 mM H_2SO_4:acetone) and three times in dry acetone and finally resuspended in sample buffer for analysis.

Promoter Tiling Array Hybridization

Input and bound fractions from two independent αUTF1 NChIP experiments were amplified using the Whole Genome Amplification kit 2 (WGA2; Sigma). Amplified material was hybridized to NimbleGen MM8 RefSeq promoter tiling arrays, containing tiled promoter regions of all RefSeq genes from 2,000 bp upstream to 500 bp downstream of the transcription start site (TSS). Design of the oligonucleotides, preparation of the slides, hybridization, and scanning of the fluorescence intensities were performed by (Roche NimbleGen, Madison, WI, www.nimblegen.com). Validations of the results by quantitative PCR (qPCR) were performed on nonamplified NChIP samples.

Promoter Tiling Array Analysis

Signals from the immunoprecipitation (IP) and "input" channel were re-expressed as $\log_2(\mathrm{IP}/\mathrm{input})$ ratios and averaged over the two technical replicates. The resulting array-wide signal distribution can be viewed as a mixture arising from two populations of tiles [27], those that are enriched and those that are nonenriched for UTF1. Let y_j ($j = 1,\ldots,n$) denote the transformed signal recorded for the tile on the array. Consistent with previous approaches [27, 28] the probability density of y_j can be modeled as a two-component mixture $f(y_j;\vec{\psi}) = \lambda_1 f_1(y_j,\vec{\theta}_1) + \lambda_2 f_2(y_j,\vec{\theta}_2)$, where $f(\cdot)$ denotes the normal density function, and $\vec{\psi} = (\lambda_1, \lambda_2, \vec{\theta}_1, \vec{\theta}_2)$ is a vector of parameters assumed a priori to be distinct. Parameter estimates are obtained in a maximum likelihood framework using the EM-algorithm [29]. This requires finding solutions to $\nabla \log L(\vec{\psi}|y) = 0$, where $L(\vec{\psi}|y) = \prod_j f(y_j;\vec{\psi})$ is the likelihood function. Once estimates, $\hat{\vec{\psi}}$ have been obtained, each y_j can be given a probable component membership via its posterior density $\tau_i(y_j;\vec{\psi}) = \lambda_i f_i(y_j,\vec{\theta}_i)/f(y_j;\vec{\psi})$, (1,2). Using these results, we control the genome-wide false-positive rate (FPR) by finding the quantile, q, that satisfies $\hat{\lambda}_1\{1 - F(q|\vec{\theta}_1)\} = \alpha$, where $F(\cdot)$, in this case, denotes the normal cumulative distribution function, and α is an arbitrarily chosen false-positive cutoff.

Peak Filtering

Because hybridized IP and input fragments are expected to span several tiles, we further required that at least six neighboring tiles exceeded the false-positive threshold to be considered as a candidate UTF1 target locus. In view of potential sequence polymorphisms between the promoter tiling array (C57Bl/6-based) and our Ola129-Hsd derived ES cells, we also allowed these enriched regions to be interrupted by maximally one nonenriched tile. Imposing these spatial requirements in this a posteriori manner differs from methods that incorporate spatial information directly into the mixture density estimation procedure, as it is the case with hidden Markov model (HMM) models. However, our peak filtering approach has the advantage of being free of modeling assumptions and of allowing for any type of correlation structure between neighboring tiles.

RNA Extraction and Array Hybridization

RNA was isolated in duplicate from wt and two independent UTF1 KD ES cell lines (UTF1 KD #1 and #2) using the Nucleospin RNA II kit (Machery-Nagel, Plesmanlaan 1d, Leiden, The Netherlands, www.mn-net.com). The RNA quality and integrity was determined using Lab-on-Chip analysis on an Agilent 2100 Bioanalyzer (Agilent Technologies, Inc., Santa Clara, CA, www.agilent.com). Biotinylated cRNA was prepared using the Illumina TotalPrep RNA Amplification Kit (Ambion, Inc., Austin, TX, www.ambion.com) starting with 500 ng total RNA and hybridized to Sentrix Mouse-6 BeadChips (Illumina, Inc., San Diego, CA, www.illumina.com). Scanning was performed on the Illumina BeadStation 500 (Illumina, Inc., San Diego, CA). Image analysis and extraction of raw expression data was performed with Illumina Beadstudio v2.3 Gene Expression software with default settings and no normalization.

Analysis of Expression Arrays and qPCR

Quantile normalization [30] was applied to the expression data from the six replicate arrays. Rank products [31] were applied to identify differentially expressed genes between the four UTF1 KD (duplicates of UTF1 KD #1 and #2) and the two wild-type (duplicates) arrays. The false discovery rate was estimated using 1,000 permutations. qPCR was performed using the MESA GREEN qPCR MasterMix Plus for SYBR Assay w/fluorescein; Eurogentec. Data were analyzed by the $2^{-\Delta\Delta Ct}$ method, using GAPDH as a reference [32].

Antibodies

The following antibodies were used: UTF1 [22]), actin (C4; MP Biomedicals, Illkirch Cedex, France, www.mpbio.com), Oct4 (H-134; Santa Cruz Biotechnology, Inc.), Troma1 (Developmental Studies Hybridoma Bank, Iowa City, Iowa, http://dshb.biology.uiowa.edu/), GAP43 (C-19; Santa Cruz Biotechnology, Inc.), GATA4 (C-20; Santa Cruz Biotechnology, Inc., Heerhugowaard, The Netherlands, www.scbt.com), Vimentin (C-20; Santa Cruz Biotechnology, Inc.), H3K4me3 (ab8580, AbCam, Cambridge, UK, www.abcam.com), H3K27me3 (07-449, Upstate, Millipore, Billerica, MA, www.millipore.com), and H3K27me1 (07-448, Upstate). Secondary antibodies for western blotting were donkey anti-rabbit IgG, horseradish peroxidase (HRP) linked (GE Healthcare, Hoevelaken, The Netherlands, www.gehealthcare.com), donkey anti-goat IgG (Santa Cruz Biotechnology, Inc.), and goat anti-mouse IgG-HRP (Santa Cruz Biotechnology, Inc.).

Gene Ontology Classification

Gene ontology (GO) analysis was performed using the Cytoscape [33] plugin BiNGO [34] and enrichment for genes in GO categories related to "Biological Process" was tested. Scores were evaluated based on the hypergeometric distribution and Benjamini and Hochberg correction for multiple testing.

Histone Extraction by MNase

To study MNase sensitivity, cells were lysed for 5 minutes on ice in 0.5% Triton X-100 in hypotonic buffer (10 mM Hepes pH 7.5, 2 mM $MgCl_2$, 15 mM NaCl, and protease inhibitors) followed by centrifugation (3,000 rpm, 25 minutes, 4°C) over a discontinuous 25%–50% (w/v) sucrose gradient. The isolated chromatin was resuspended at 1 mg/ml in digestion buffer and incubated at 37°C with 0.048 U/ml of MNase (Sigma). The MNase reaction was terminated by addition of 5 mM EDTA and incubation on ice. Extracted histones were isolated by centrifugation (14,000 rpm, 10 minutes, 4°C).

Subsequently, DNA was isolated by phenol/chloroform extraction as described earlier.

Southern Blotting

Genomic DNA was isolated from IB10 ES cells and digested with a methylation-sensitive restriction enzyme (HpaII) or its methylation-insensitive isoschizomer (MspI) as a control. Five micrograms of digested genomic DNA was loaded on 2% agarose gels and southern blotting analysis was performed. Minor satellite repeats were recognized by a 162 bp probe, pCR4 Min5-1 [35] that was labeled and detected using the DIG High Prime DNA Labeling and Detection Starter Kit II (Roche, Woerden, The Netherlands, www.roche.com).

RESULTS

Genome-Wide Promoter Occupation by UTF1

We previously reported that both mouse and human UTF1 are tightly chromatin-associated proteins with core histone-like dynamics, transcriptional repressor activity and that UTF1 is required for proper differentiation of mouse ES cells [22, 23]. This tight interaction between UTF1 and chromatin was confirmed using mass-spectrometry analysis of immune precipitations of endogenous UTF1 or stably expressed green fluorescent protein-UTF1 (GFP-UTF1) as a direct interaction with the core histones H2A, H2B, H3, and H4 was detected (Supporting Information Figure S1).

To identify the target genes of UTF1, we performed αUTF1 NChIP on ES cells [26]. Bound (IP) and input samples were amplified and hybridized to NimbleGen promoter tiling arrays. Using a mixture modeling approach, we classified array signals corresponding to enriched tiles (Supporting Information Figure S2, [28]). Promoters with six consecutive enriched tiles, interrupted by maximally one nonenriched tile, were designated as UTF1 targets. This resulted in the identification of 1,467 tiled regions and due to multiple gene annotations to several of the tiled regions, these regions mapped to 1,735 annotated genes (FPR $<$ 0.01; Fig. 1A, Supporting Information Table S1). To investigate the distribution of UTF1 binding sites relative to the TSS, we plotted the density of enriched tiles against their distance from the TSS. Although UTF1 occupancy occurred throughout the tiled promoters, there was a clear bias toward regions immediately flanking the TSS (Fig. 1B). The observed drop off in binding around $-1{,}800$ and $+300$ is caused by our definition of a UTF1 binding site (the center of five consecutive enriched tiles), which results in a decrease in UTF1 binding sites close to the start and end of tiled regions. A consensus UTF1-interaction motif was not detected in the enriched regions using Multiple EM for Motif Elicitation (MEME) [36]. However, UTF1-enriched regions are not randomly distributed throughout the genome. For chromosome X, the number of UTF1-bound regions was significantly low, whereas significantly more UTF1-bound regions were observed on chromosomes 11, 17, and Y (Supporting Information Figure S3). A closer inspection of the 1,467 UTF1 target regions led to the identification of two distinct UTF1-occupancy patterns: either widespread (290 tiled regions; e.g., Mid1, MGC107098 and Ssty1; Supporting Information Figure S4) or as a peak on a limited number of tiles (1177 regions; e.g., Hist2h3c1; Fig. 1C, Supporting Information Figure S4).

GO analysis revealed that UTF1-occupied genes are involved in chromatin assembly, DNA packaging, nucleosome assembly, and protein-DNA complex assembly (Fig. 1D). Although not a significantly enriched GO category, many UTF1 target genes are involved in spermatogenesis (a significant enrichment on the Y chromosome was observed, Supporting Information Figure S3). In addition to these Y-linked spermatogenesis genes, UTF1 is also associated with promoter regions of several spermatogenesis genes located on autosomal chromosomes. The significant GO categories contained many histone genes. In the mouse, histone genes are located in three clusters on chromosomes 3, 11 and 13 [37], and all three clusters contained several UTF1 targets. UTF1 occupation of the Hist1 cluster on chromosome 13 and on a part of the Y chromosome containing many spermatogenesis genes is shown in Supporting Information Figure S5.

An extensive network of transcription factors required for ES cell pluripotency, with Oct4, Sox2, and Nanog as core members, has been investigated extensively [38–43]. To determine whether UTF1 and self-renewal/reprogramming factors regulate common sets of genes, we compared UTF1 target genes with the targets of Nanog, Sox2, Dax1, Nac1, Oct4, Klf4, Zfp281, Rex1, and c-Myc [41]. We found a significant overlap ($p < .01$) between UTF1 and Nanog, Oct4, Klf4, Rex1, and c-Myc target genes (Fig. 1E).

Summarizing, ChIP-on-chip analysis led to the identification of 1,467 UTF1-enriched regions, mapping to 1,735 genes, with a nonrandom genome-wide distribution. A remarkable enrichment of UTF1 was observed on spermatogenesis-linked genes on the Y-chromosome.

Gene Expression Analysis in UTF1-Depleted Cells

We previously demonstrated that UTF1 represses reporter gene activity [22, 23]. To investigate whether UTF1 regulates ES cell gene expression, we compared the gene expression profiles of wild-type and two independent stable UTF1 KD ES cell lines. Clustering analysis showed that UTF1 KD results in a reproducible change in expression profile (Fig. 2A). As expected, among the differentially expressed transcripts, UTF1 is strongly downregulated in UTF1 KD ES cells (see also Supporting Information Figure S6). Overall, 1,090 transcripts were significantly upregulated (Supporting Information Table S2) and 131 transcripts significantly downregulated (Supporting Information Table S3) in UTF1-depleted versus wild-type ES cells (FPR $<$ 0.05; Fig. 2B). Of the 131 genes downregulated in UTF1 KD ES cells, seven are imprinted genes. Significant downregulation of H19, Igf2, and p57 and upregulation of Hist1h2bc, Nanog, Esrrb, Klf4, and Rhox2 transcript levels was confirmed using qPCR ($p < .05$, Fig. 2C). GO analysis of all downregulated genes indicated an overrepresentation of genes involved in developmental processes, like blood vessel development, tube development, and pariaxal mesoderm morphogenesis (Fig. 2D). GO analysis of the significantly upregulated genes indicated that many of these genes are involved in regulation of gene expression, metabolism, and processing of RNA (Fig. 2E). Among the upregulated genes, we also identified a set of genes involved in early embryonic development and ES cell function, like Nanog, Esrrb, Nodal, and Klf4. Although not assigned to this particular GO category, Wnt3A, a protein involved in maintaining ES cell pluripotency [44] is also upregulated in the absence of UTF1.

Differentiation and Colony Formation by UTF1 KD ES Cells

We determined if the upregulation of these self-renewal/pluripotency genes affected LIF dependency, DMSO- or RA-induced differentiation, and colony formation activity of UTF1 KD ES cells. On LIF withdrawal, the morphology of both wild-type and UTF1 KD ES cells rapidly changed (Fig. 3A). To determine potential differences in differentiation kinetics, expression levels of Oct4 and UTF1 were monitored after LIF withdrawal. Already 2 days after removal of LIF, Oct4 was below detection levels in wild-type ES cells and UTF1 expression levels sharply

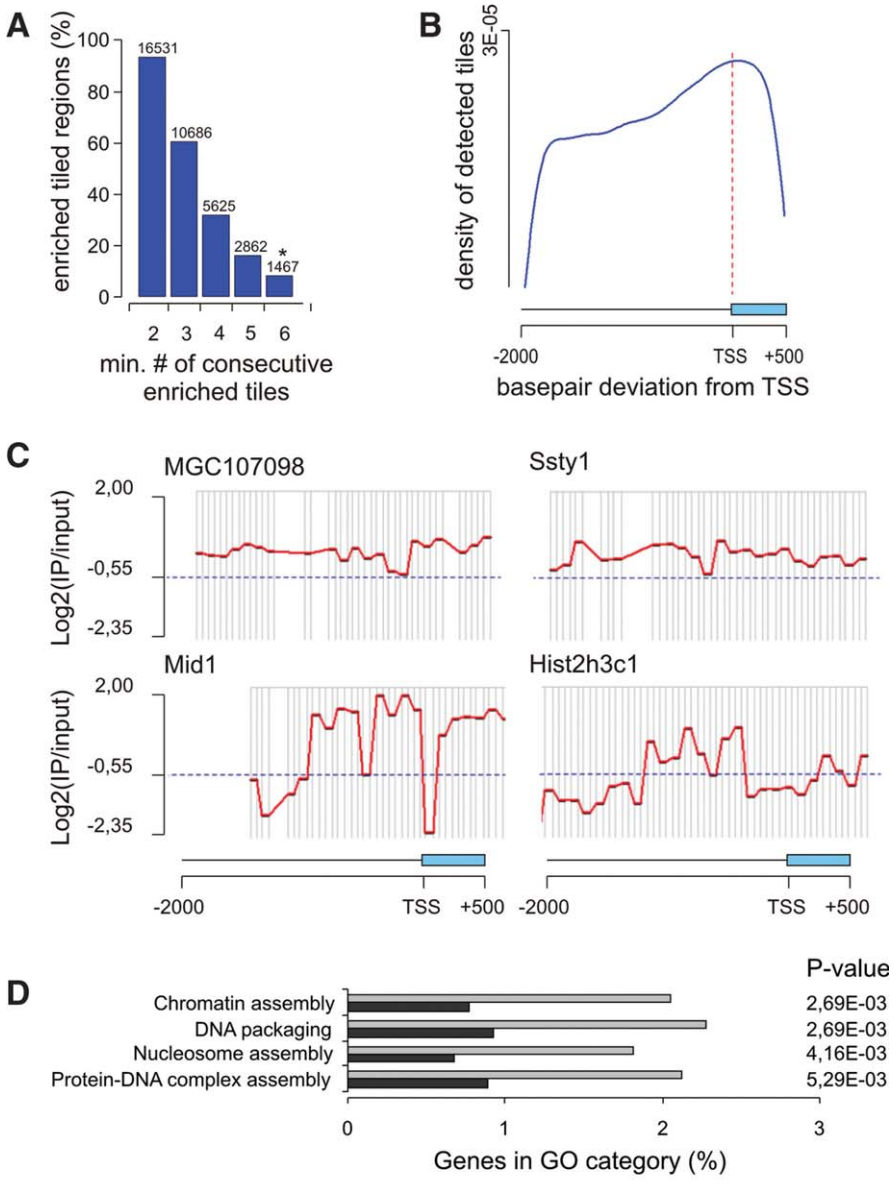

E

	targets	overlap	P-value
Nanog	1284	136	**0.01**
Sox2	819	77	0.25
Dax1	1754	165	0.17
Nac1	804	76	0.24
Oct4	783	99	**0.0001**
Klf4	1790	181	**0.01**
Zfp281	601	50	0.66
Rex1	1543	188	**<0.0001**
c-Myc	3542	415	**<0.0001**

Figure 1. Global mapping of undifferentiated embryonic cell transcription factor 1 (UTF1) target genes. **(A):** Identification of enriched tiled regions. The percentages of enriched tiled regions are shown based on an increasing amount of enriched consecutive tiles, allowing for one nonenriched tile within the consecutive sequence of enriched tiles (indicated on the *x*-axis). The asterisk shows the set of enriched promoters that was used for further analyses. **(B):** Density of enriched tiles within enriched promoters. Their position in bp relative to the TSS is indicated. On the promoter tiling arrays, maximally −2000 bp to +500 in relation to the TSS was tiled and this region is indicated. **(C):** Occupation of UTF1 over selected enriched promoter regions. Individual tiles are indicated by gray vertical lines. The false-positive cutoff is indicated by the blue dotted lines. **(D):** GO classifications of genes whose promoter is occupied by UTF1. The percentage of genes belonging to each category within the UTF1-bound population is indicated (light gray bars) as well as the percentage expected based on chance (dark gray bars). **(E):** Comparison of UTF1 target genes with the pluripotency transcription factor network. The number of promoters bound by each factor (targets) and the overlapping number of UTF1 target promoters (overlap) of a total of 1,736 UTF1 target promoters are depicted and *p* values were determined using bootstrap testing. Abbreviations: GO, gene ontology; TSS, transcription start site.

decreased, but still was detectable throughout the time points analyzed. However, in UTF1 KD ES cells, Oct4 was still expressed up to 4 days after LIF removal (Fig. 3A). Colony formation efficiency of IB10 and UTF1 KD ES cells was determined by seeding cells in 10-cm Ø dishes in triplicate, followed by Giemsa staining and colony counting. UTF1 KD ES cells displayed an approximately twofold enhanced colony formation compared with wild-type cells (Fig. 3B).

RA treatment induced differentiation in wt and UTF1 KD ES cells with similar kinetics, confirming previous observations obtained in embryoid bodies ([22]; Fig. 3C). We also treated wild-type and UTF1 KD ES cells with DMSO and followed differentiation. Like after LIF withdrawal, a delayed differentiation of UTF1 KD ES cells was observed as Troma1 and Vimentin were detected after 2 days in wild-type ES cells, but only after 5 and 10 days respectively in UTF1 KD

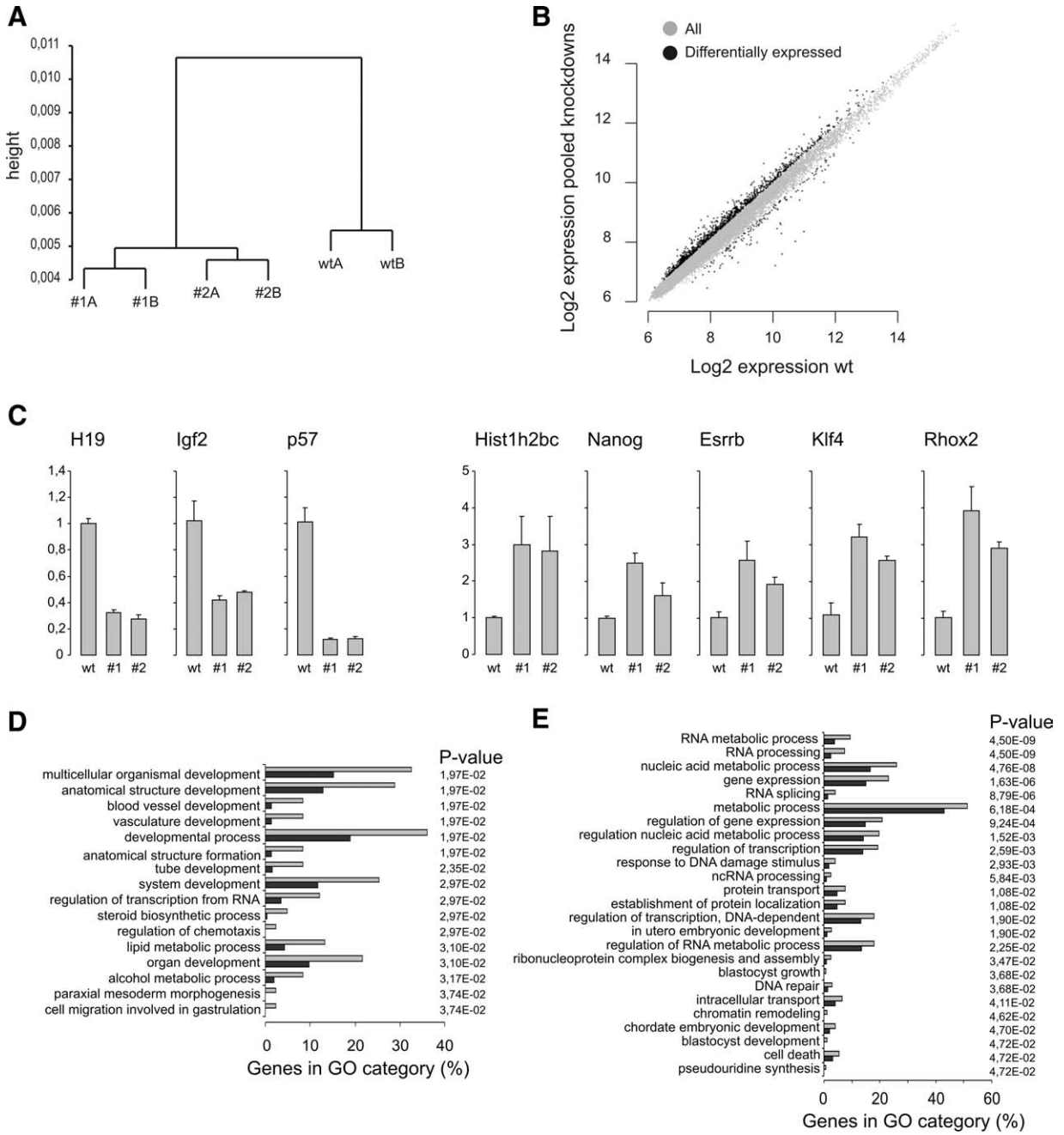

Figure 2. The effect of undifferentiated embryonic cell transcription factor 1 (UTF1) knock down (KD) on embryonic stem (ES) cell gene expression. **(A):** Hierarchical clustering of expression data of biological replicates (A and B) of wt and two independent UTF1 knock down (#1 and #2) embryonic stem cell lines. Pearson's correlation was used for distance measurement. **(B):** Log2 expression level of all probes in wild-type versus UTF1 KD ES cells. All probes are indicated by gray dots and the probes with significant differential expression are indicated with black dots. **(C):** Validation of gene expression changes by reverse transcriptase-quantitative polymerase chain reaction (RT-qPCR) for a selection of downregulated (H19, Igf2, and p57) and upregulated (Hist1h2bc, Nanog, Essrb, Klf4, and Rhox2) genes. cDNA was prepared from wild-type and UTF1 KD ES cells. Data were analyzed by the $2^{-\Delta\Delta Ct}$ method, using glyceraldehyde 3-phosphate dehydrogenase as a reference [32]. All genes depicted were significantly downregulated or upregulated ($p < .05$). **(D):** Selected gene ontology classifications of genes that are downregulated in UTF1 KD ES cells. The percentage of genes belonging to each category within the downregulated population is indicated (light gray bars) as well as the percentage expected based on chance (dark gray bars). **(E):** Selected gene ontology classifications of genes that are upregulated in UTF1 KD ES cells. The percentage of genes belonging to each category within the upregulated population is indicated (light gray bars) as well as the percentage expected based on chance (dark gray bars). The level of UTF1 KD in the IB10 ES cells used is shown in Supporting Information Figure S6. Abbreviations: GO, gene ontology; wt, wild-type; wtA, wild-type A; wtB, wild-type B.

ES cells (Fig. 3D). GATA4 was detected after 10 days in wild-type ES cells, but not in the UTF1 KD lines. Summarizing, these data show that UTF1 KD ES cells do differentiate on LIF withdrawal or when treated with DMSO or RA, albeit with slower kinetics (LIF and DMSO) than wild-type ES cells. These findings are in agreement with our previous observations that embryoid bodies from UTF1 KD ES cells remained largely alkaline phosphatase positive and expressed

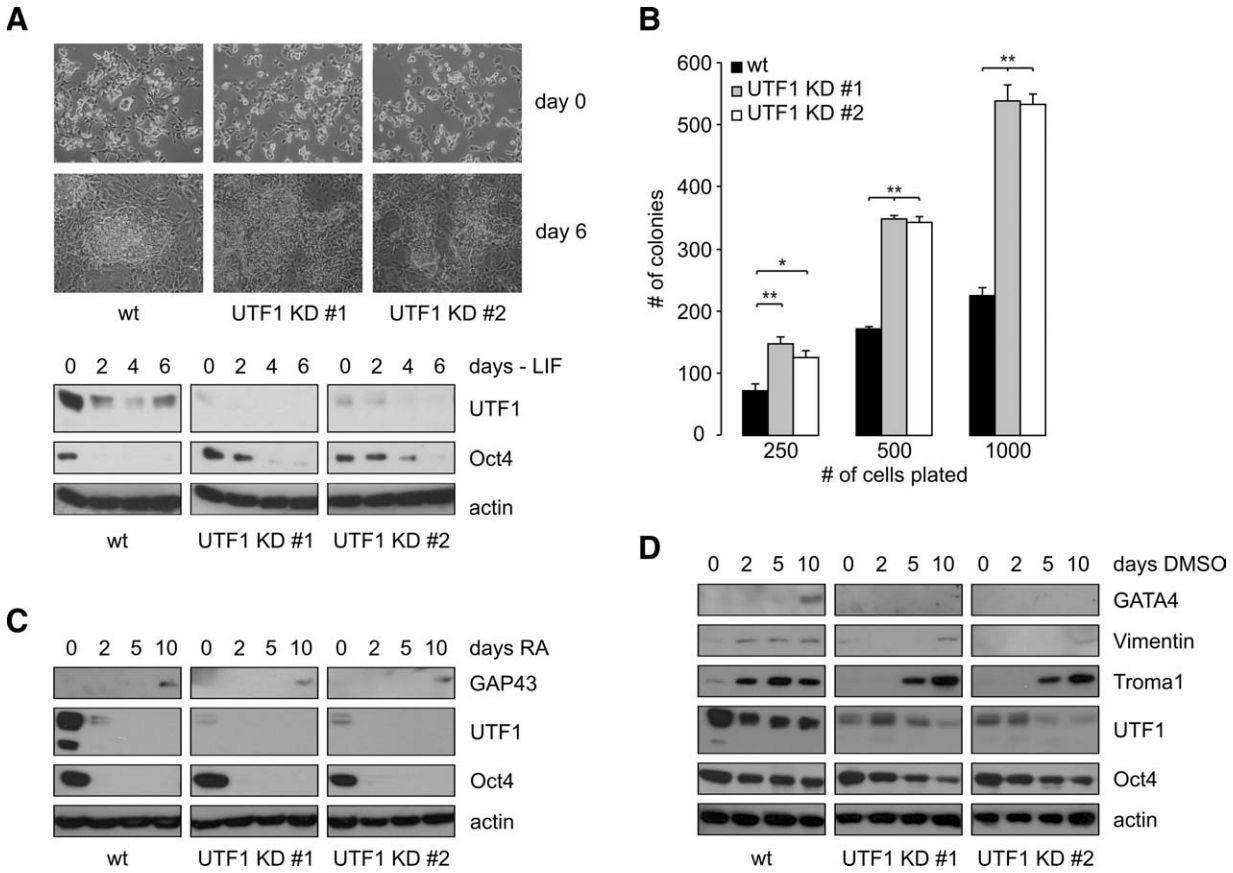

Figure 3. Differentiation and colony formation of wild-type and UTF1 KD IB10 embryonic stem (ES) cells. **(A):** Phase-contrast images and western blots of wt and UTF1 knock down (#1 and #2) ES cells after LIF withdrawal. Cell lysates were analyzed with antibodies against UTF1, Oct 4, and actin as a loading control. **(B):** Wild-type and UTF1 KD ES cells were plated at different densities and after 8 days colonies were counted (*, $p < .05$; **, $p < .01$). **(C, D):** RA- and DMSO-induced differentiation (0, 2, 5, and 10 days) of wt and UTF1 KD ES cells. Cell lysates were analyzed using the antibodies indicated. Abbreviations: DMSO, dimethyl sulfoxide; GAP43, growth associated protein 43; LIF, leukemia inhibitory factor; RA, retinoic acid; UTF1 KD, undifferentiated embryonic cell transcription factor 1 knock down; wt, wild-type.

some differentiation markers, but delayed compared with wild-type ES cells [22].

Summarizing, these results suggest that (a fraction of the) UTF1 KD ES cells have an increased self-renewal activity and are somewhat refractory to or delayed in differentiation.

Differentially Expressed UTF1 Targets

To determine the relation between UTF1 occupation and expression, gene expression and ChIP-on chip data sets were compared. Interestingly, most UTF1-occupied genes are in the lower range of expression levels (Supporting Information Figure S7A). Of the 1,735 identified UTF1 target genes, 109 genes ($p = .0001$, Supporting Information Figure S8) displayed altered expression levels in UTF1-depleted ES cells of which 101 were upregulated (Supporting Information Figure S7B). In summary, these data show that UTF1 KD results in differential, mainly increased expression levels of approximately 1,200 transcripts, and a significant number (109 genes) is bound by UTF1.

Chromatin Changes in UTF1 KD ES Cells

In view of the fact that the majority of UTF1 target genes are silent or expressed at low levels and that knock down of UTF1 primarily results in increased expression of those targets, we determined whether global levels of histone modifications associated with active or silent chromatin were altered in UTF1-depleted ES cells. No differences in histone modification levels were observed between wild-type, *Renilla* luciferase, and UTF1 KD ES cell lines (Supporting Information Figure S9).

To determine if UTF1-associated chromatin is enriched for repressive histone modifications, N-ChIP experiments were performed on P19CL6 cells using an αUTF1 antibody and the precipitated histones were analyzed. Coprecipitation of core histones with UTF1 was observed, but not with preimmune serum (Fig. 4A). To address whether UTF1-bound chromatin is enriched for repressive or active histone modifications, and whether that changes on differentiation of P19CL6 cells, we treated P19CL6 cells with 1% DMSO for 0, 2, and 4 days. The tight association of UTF1 with chromatin does not change during differentiation, as UTF1 was still detected in the tightly DNA-associated ammonium sulfate fraction in subnuclear fractionations of DMSO-differentiated P19CL6 cells (Supporting Information Figure S10). Next, αUTF1 NChIPs were performed and equal amounts of histones for input, unbound, and bound fractions were analyzed for H3K27me1, H3K27me3, and H3K4me3 (Fig. 4B, 4C). Strikingly, UTF1-associated chromatin was highly enriched for H3K27me3, but much less for H3K27me1 and H3K4me3 (Fig. 4B, 4C). During differentiation, we observed an intermediate enrichment (day 2) and no enrichment (day 4) for H3K27me3 in UTF1-precipitated chromatin. H3K27me1 and H3K4me3 levels were approximately twofold enriched at day 0, and where H3K27me1 enrichment decreased during differentiation, H3K4me3 enrichment levels remained

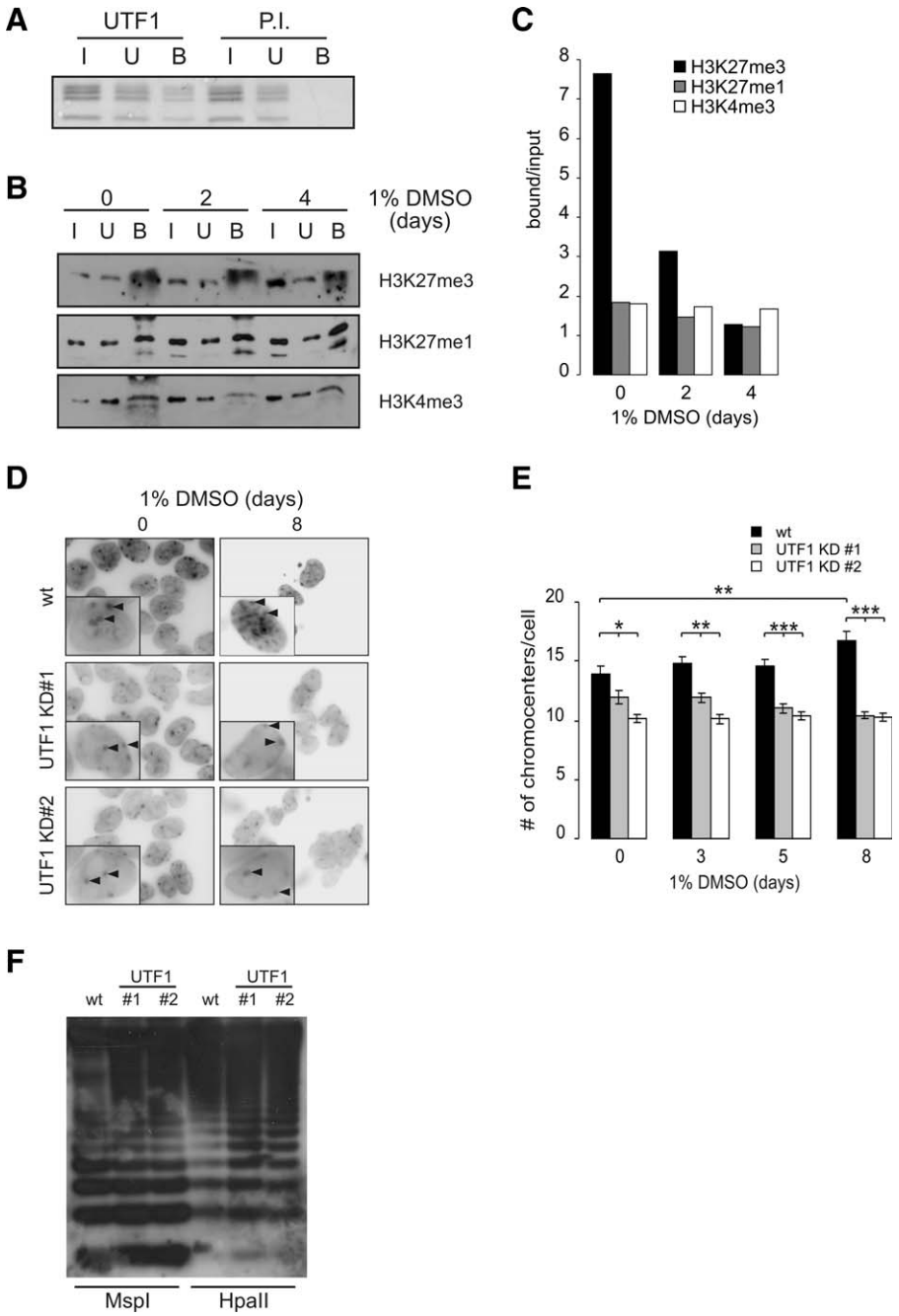

Figure 4. UTF1 depletion results in a more open chromatin structure. **(A):** Native chromatin immunoprecipitation with a UTF1 antibody or a P.I. I, U, and B samples were separated using polyacrylamide gel electrophoresis (PAGE) and stained with coomassie. **(B):** Native chromatin immunoprecipitation on P19CL6 cells treated for 0, 2, or 4 days with 1% dimethyl sulfoxide (DMSO). Equal amounts of histones from I, U, and B samples were loaded and stained with the indicated antibodies. **(C):** Quantification of western blots shown in **(A)**. **(D):** Immunofluorescent analysis of wt and UTF1 KD (UTF1 KD#1 and #2) P19CL6 cells. Cells were differentiated with 1% DMSO for 8 days. After 0 and 8 days, cells were fixed with paraformaldehyde and stained with 4′,6-diamidino-2-phenylindole (DAPI). Images were grayscaled and inverted. Insets: magnification of a single cell and arrowheads indicate examples of chromocenters. The level of UTF1 KD in the P19CL6 cells used is shown in Supporting Information Figure S12. **(E):** At day 0, 3, 5, and 8 of DMSO treatment, the number of DAPI dense chromocenters was determined in at least 40 cells per time point. The average number of chromocenters per cell is indicated with the standard error of mean. **(F):** Southern blot analysis of genomic DNA isolated from wild-type and UTF1 KD (#1 and #2) IB10 ES cells and digested using a methylation-sensitive restriction enzyme (HpaII) and its methylation-insensitive isoschizomer (MspI) as a control. The blot was hybridized with a probe specific for minor satellite repeats. The level of UTF1 KD in the IB10 ES cells used is shown in Figure 5B. Abbreviations: B, bound sample; DMSO, dimethyl sulfoxide; I, input sample; P.I., preimmune control; U, unbound sample; UTF1, undifferentiated embryonic cell transcription factor 1; UTF1 KD, undifferentiated embryonic cell transcription factor 1 knock down; wt, wild-type.

unaltered. During P19CL6 differentiation, H3K27me3 levels increased (compare the H3K27me3 levels in the input lanes in panel 3B) and UTF1 levels decreased, explaining a progressive loss of H3K27me3 enrichment in UTF1-precipitated chromatin during differentiation.

We investigated whether the enrichment of UTF1-associated chromatin for repressive histone modifications was reflected by overlapping subnuclear distributions. The localization of H3K27me3, H3K4me3, H3K9me3, H4K20me3, H2B-GFP, and endogenous UTF1 was determined in P19CL6 cells stably expressing either GFP-UTF1 or monomeric red fluorescent protein-UTF1 (mRFP-UTF1) (Supporting Information Figure S11). Among the investigated histone modifications, the most pronounced colocalization was observed between UTF1 and H3K27me3 (Pearson's correlation coefficient, $R = .18$) and H3K4me3 ($R = .10$), where the heterochromatin marks H3K9me3 and H4K20me3 are poorly colocalized with UTF1 ($R = -0.01$ and $R = 0.01$ respectively). However, the line scans indicate that the chromocenters, where H3K9me3 and H4K20me3 levels peak, are not devoid of GFP-UTF1. As expected, GFP-UTF1 and endogenous UTF1 showed extensive colocalization ($R = .63$) and a clearly overlapping distribution was observed between mRFP-UTF1 and H2B-GFP ($R = .68$).

To determine a possible role for UTF1 in the organization of higher order chromatin structures in P19CL6 cells and during their differentiation, we studied chromocenters in wild-type and UTF1 KD P19CL6 cells. In the mouse nucleus, pericentric heterochromatin, composed of major and minor satellite repeats, tends to cluster into chromocenters [45]. Chromocenters are characterized by the presence of histone modifications H3K9me3 and H4K20me3, HP1, and the absence of H3K4me3. The number of chromocenters, as

identified by DAPI-dense regions, was determined after 0, 3, 5, and 8 days of differentiation (Fig. 4D, 4E). Undifferentiated UTF1 KD cells (day 0), contained a little less, (but structurally similar) chromocenters than wild-type cells ($p < .05$ for UTF1 KD #1 and $p < .01$ for #2). During differentiation, the number of chromocenters in wild-type cells increased significantly ($p < .01$ between day 0 and day 8), which is in agreement with previously published data [9, 11]. In both UTF1 KD lines, this increase was not observed, most likely reflecting the differentiation defect of UTF1 KD cells. Upregulation and downregulation of pluripotency and differentiation markers during P19CL6 differentiation was confirmed using western blotting (Supporting Information Figure S12). To determine if chromocenter-specific histone modifications were altered in the UTF1 KD cells, heterochromatin markers H3K9me3, H4K20me3, and HP1γ and the euchromatic histone modification H3K4me3 were analyzed using immunofluorescence (Supporting Information Figure S13). As expected, in both wild-type and UTF1 KD P19CL6 cells, a distinct accumulation of H3K9me3, H4K20me3, and HP1γ was observed at the chromocenters. (Supporting Information Figure S13).

Another epigenetic characteristic of chromocenters is CpG methylation of the centromeric minor and major satellite repeats. DNA methylation levels of the pericentric heterochromatin were determined in wild-type and UTF1 KD ES cells. Using methylation-sensitive restriction enzymes and southern blotting, a reduction in DNA methylation levels at the minor satellite repeats in UTF1 KD cells was observed (Fig. 4F).

These data show that despite the fact that the chromocenter structure and histone mark content are not altered in UTF1 KD cells, their numbers are significantly reduced and do not increase during differentiation like in wild-type cells. Interestingly, the centromeric minor satellites show a reduction in CpG methylation levels.

MNase Sensitivity in UTF1 KD ES Cells

In view of the observations that UTF1 depletion resulted in an increased expression of a large number of transcripts, we hypothesized that UTF1 is involved in the regulation of chromatin structure in ES cells. To monitor the nuclear chromatin organization, the rate of core histone release from UTF1 KD and wild-type ES cell nuclei on MNase digestion was measured (Fig. 5A). To calculate the percentage of histones extracted, the amount of released histones was normalized to their respective input samples. After 30 minutes of MNase treatment, approximately 30% of total histones was released from wild-type ES cells (Fig. 5A). Interestingly, in UTF1 KD ES cells, the extraction percentage was almost doubled to 50%. Efficient UTF1 KD was confirmed by western blotting of input samples, Oct4 staining confirmed pluripotency and actin was used as a loading control (Fig. 5B). Subsequent analysis of release of histones carrying specific modifications (H3K4me3 and H3K27me3) gave similar results: a drastic increase in extraction efficiency in UTF1 KD compared with wild-type cells. H3K4me3 extraction efficiency increased from 25% to 40% and for H3K27me3 an increase from 20% to 50% was observed (Fig. 5A). These data indicate that UTF1-depleted chromatin is more sensitive to MNase treatment, resulting in enhanced release of core histones. This is supported by the fact that only very little UTF1 is detected in the MNase-treated wild-type ES cell samples (Fig. 5C), indicating that UTF1-enriched chromatin is more resistant against MNase digestion.

To study the effect of UTF1 on MNase sensitivity in the context of its own target genes, genomic DNA was isolated from MNase-extracted ES cells. Subsequently, qPCR was performed using primer sets directed against UTF1-enriched regions, identified in the ChIP-on-chip analysis. In contrast to wild-type cells, a number of UTF1-bound regions (MGC107098, Sly, Ssty1) could not be amplified after MNase treatment of UTF1 KD cells, indicating that UTF1 protects these sites from degradation in wild-type cells (Fig. 5D). Other UTF1 target genes display intermediate (Mid1) or wild-type level (Hist2h3c1 and Hist3h2ba) sensitivity to MNase treatment. Summarizing, these data indicate a structural role for UTF1 in ES cell chromatin organization, most likely by contributing to a condensed chromatin structure at its target loci, thereby preventing aberrant transcription.

Discussion

We previously reported that UTF1 is a tightly chromatin-associated protein with core histone-like properties [22]. We consistently identified core histones as UTF1 coprecipitating proteins, also after benzonase treatment, indicating that these histones were not obtained through inadvertent coprecipitation of large nucleosome-containing genomic DNA fragments.

To identify UTF1 target genes across the genome, we used a ChIP-on-chip approach, leading to the identification of >1,700 UTF1 target genes. UTF1 is not randomly distributed over the DNA, as a clear enrichment on chromosomes 11, 17, and Y was observed. Furthermore, the pattern of UTF1 occupancy on many target genes is peak-shaped (1,177 of 1,467 regions), indicating a specific targeting of UTF1 within these regions. In addition to this peak-shaped pattern, a wide-spread occupancy on many target genes was observed as well (290 regions). How far UTF1 occupancy spreads into the flanking chromatin is unclear, but this suggests that UTF1 binding is not restricted to the promoter region of genes. Within UTF1-enriched genomic regions no specific UTF1 binding motif could be identified. Probably factors other than the DNA sequence are involved in targeting UTF1 to its sites of affinity.

Interestingly, when comparing the UTF1 target genes with those of various transcription factors involved in ES self-renewal and somatic reprogramming as reported by Kim and coworkers, a significant overlap with target genes of Nanog, Oct4, Klf-4, Rex1, and c-Myc was observed [41]. This observation supports a role for UTF1 during somatic reprogramming as was reported by Zhao et al. who showed that UTF1 increases the efficiency of iPS cell generation and leads to more ES-like iPS clones [24]. Although a significant overlap was observed between UTF1 and Nanog and Oct4 target genes, UTF1 is probably not involved in self-renewal, as UTF1-depleted ES cells are able to self-renew but are defective in differentiation [22] and have decreased tumorigenicity in teratoma formation (our unpublished data, [46]).

During embryonic development, UTF1 is expressed in primordial germ cells [47]. In the testis, UTF1 expression is restricted to the spermatogonial stem cells [48]. In line with these data, we observed extensive enrichment of UTF1 on genes involved in spermatogenesis, both on the Y chromosome and autosomes, confirming a role for UTF1 in gonadal development and spermatogenesis.

By expression profiling, we determined that UTF1 KD in ES cells results in differential expression of >1,200 genes of which 90% was upregulated. The large number of upregulated genes in combination with the fact that many significant GO terms were related to the process of gene expression, indicate that UTF1 KD ES cells are in a state of higher transcriptional activity. Interestingly, UTF1-occupied genes in general display a very low transcriptional activity, which is in agreement with our earlier findings that UTF1 is a transcriptional repressor [22]. The fact that removal of UTF1 is not sufficient for full

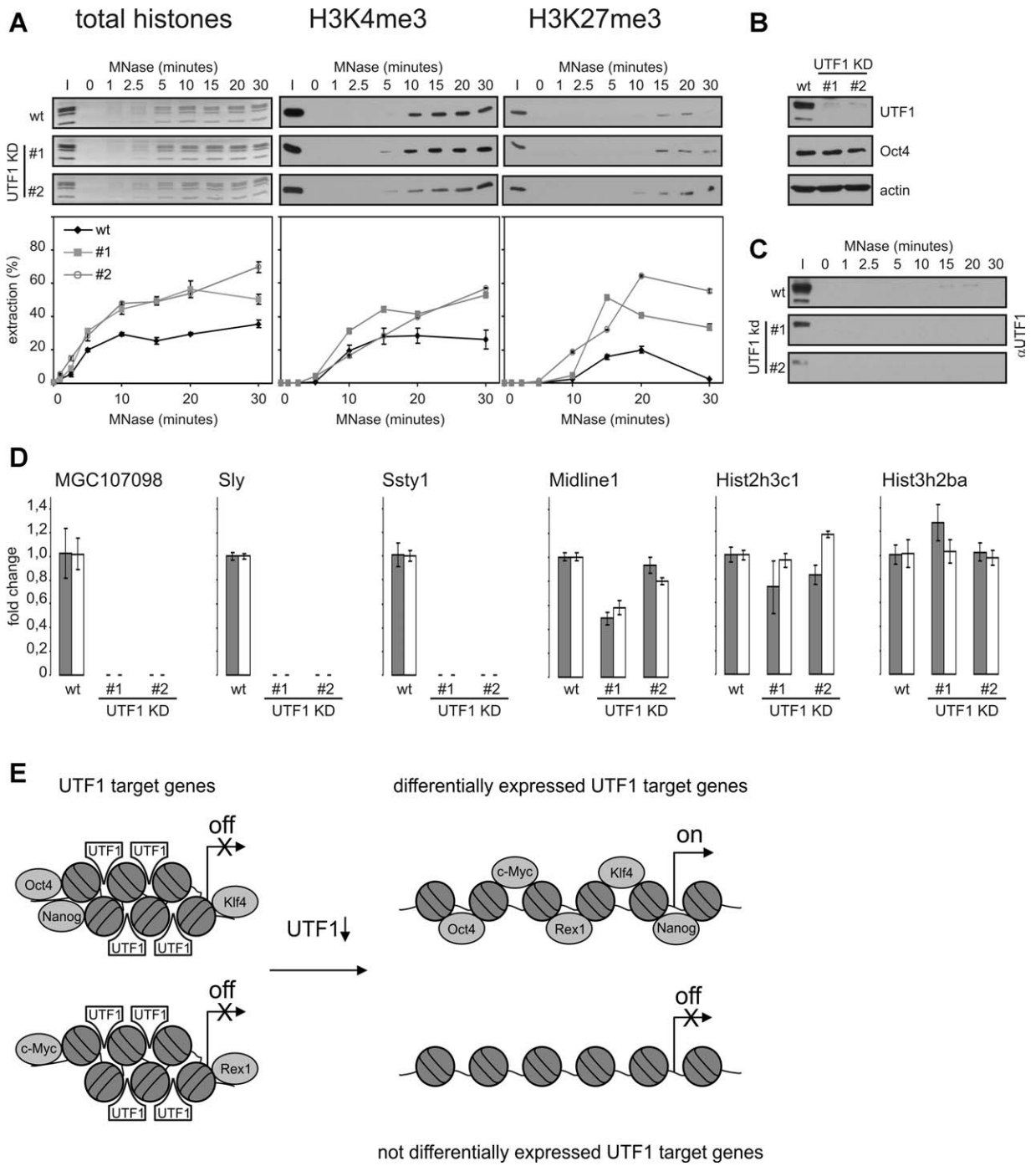

Figure 5. UTF1 depletion results in increased MNase sensitivity. **(A):** Coomassie analysis of MNase-treated chromatin isolated from wt and UTF1 KD (UTF1 KD#1 and #2) IB10 cells. Histones were quantified, and the amount of extracted (modified) histones was calculated relative to the input and is depicted as % extraction with standard deviations (wt: black line with diamonds, UTF1 KD #1: gray line with squares, UTF1 KD #2: gray line with open circles). Samples were also analyzed with antibodies against H3K4me3 (middle panel) or H3K27me3 (right panel). Three independent experiments were performed and a representative experiment is shown **(B)** UTF1, Oct4, and actin levels in wild-type and UTF1 KD ES cells at time of chromatin extraction. **(C):** Western blot analysis of UTF1 in input and MNase-treated samples of wt and UTF1 KD IB10 cells. **(D):** Quantitative PCR analysis of UTF1-enriched promoter regions. Fold change for 2.5 minutes (gray bars) and 20 minutes (white bars) MNase-treated samples was calculated relative to GAPDH and relative to wild-type. **(E):** Proposed model for UTF1 function. UTF1 target genes are often co-occupied by combinations of the indicated transcription factors and generally expressed at low levels in embryonic stem cells. Downregulation of UTF1 might result in chromatin decondensation and increased expression of a significant number of target genes. A significant number of these genes are targets of the indicated transcription factors, where other UTF1 target genes, although decondensed, are not differentially expressed on UTF1 downregulation. Abbreviations: I, input; MNase, micrococcal nuclease; UTF1, undifferentiated embryonic cell transcription factor 1; UTF1 KD, undifferentiated embryonic cell transcription factor 1 knock down; wt, wild-type.

activation of all its targets genes could be caused by the fact that, apart from UTF1, other transcriptional repressors keep the transcriptional activity low. Otherwise, transcription factors required for their transcriptional activation may not yet be expressed in undifferentiated ES cells. Finally, the increase in transcriptional activity of UTF1 target genes may also be a consequence of local chromatin decondensation upon UTF1 depletion. As a potential regulator of chromatin condensation, UTF1 could be involved in the reduction of transcriptional noise, which has been proposed to be important to minimize transcription of differentiation inducing genes [21, 49].

Among the genes downregulated in UTF1 KD ES cells, several imprinted genes were present. It has been reported that expression of imprinted genes varies greatly between individual ES cell subclones and that the methylation patterns of imprinted genes is unstable in ES cells [50, 51]. Nevertheless, we consistently observed a downregulated expression of these imprinted genes compared with wild-type ES cells in all UTF1-depleted ES subclones tested. Whether UTF1 depletion affects imprinted gene expression by deregulation of methylation of regulatory elements, similar to the observed hypomethylation of pericentric heterochromatin in UTF1 KD cells, remains to be investigated.

A relatively small, but significant ($p = .0001$) fraction of the UTF1-occupied genes is differentially expressed (109 of 1,221). It is possible that a part of the differentially expressed genes are not direct UTF1 targets, but are altered in their expression as a secondary consequence of altered expression of UTF1 target genes. Furthermore, in the ChIP-on-chip assays, promoter tiling arrays were used, maximally covering −2,000 to +500 bp in relation to the TSS. Genes occupied by UTF1 outside this tiled region will not have been identified as UTF1 target genes in our experiments, possibly leading to an underestimation of the number of UTF1 targets in the differentially expressed genes.

A more general role for UTF1 in regulating ES cell chromatin condensation is suggested by the enhanced MNase sensitivity and reduced number of chromocenters in UTF1 KD cells. Chromatin in ES cells is decondensed and globally, albeit at low levels, transcriptionally hyperactive, which is postulated to contribute to their plasticity and pluripotency [13]. Although the exact role of chromatin structure in ES cell pluripotency is unknown, ES cells that lack critical chromatin regulators exhibit differentiation defects indicating a role for these proteins during differentiation initiation and chromatin remodeling during lineage specification [52]. Recently, the chromatin remodeling factor Chd1 was reported to induce a decondensed chromatin state in ES cells and knock down resulted in loss of pluripotency [14].

Conclusion

In summary, the data presented here show that UTF1 is an important chromatin component in ES cells. UTF1 binds many target genes in ES cells and UTF1 KD in ES cells resulted in increased gene expression of a large set of genes and differentiation defects. We propose that UTF1 is essential to preclude superfluous decondensation of ES cell chromatin and thereby might contribute to the prevention of aberrant gene expression.

Acknowledgments

We thank Michel Meijer for deconvolution of confocal images and Dr. Pernette J. Verschure for stimulating discussions concerning chromocenters. This work was supported by the Groningen Biomolecular Sciences and Biotechnology Institute and the Netherlands Proteomics Initiative. V.v.d.B. was funded by Dutch Cancer Society Grant RUG 2007-3729. S.M.K. is currently affiliated with the Biotech Research and Innovation Centre (BRIC), University of Copenhagen, Ole Maaløes Vej 5, 2200 Copenhagen, Denmark; V.v.d.B. is currently affiliated with the Department of Hematology, University Medical Center Groningen, Groningen, The Netherlands.

Disclosure of Potential Conflicts of Interest

The authors indicate no potential conflicts of interest.

References

1 van Driel R, Fransz PF, Verschure PJ. The eukaryotic genome: A system regulated at different hierarchical levels. J Cell Sci 2003;116:4067–4075.
2 Misteli T. Beyond the sequence: Cellular organization of genome function Cell 2007;128:787–800.
3 Kouzarides T. Chromatin modifications and their function Cell 2007; 128:693–705.
4 Bernstein BE, Mikkelsen TS, Xie X et al. A bivalent chromatin structure marks key developmental genes in embryonic stem cells. Cell 2006;125:315–326.
5 Jorgensen HF, Giadrossi S, Casanova M et al. Stem cells primed for action: Polycomb repressive complexes restrain the expression of lineage-specific regulators in embryonic stem cells. Cell Cycle 2006;5:1411–1414.
6 Boyer LA, Mathur D, Jaenisch R. Molecular control of pluripotency. Curr Opin Genet Dev 2006;16:455–462.
7 Chen L, Daley GQ. Molecular basis of pluripotency. Hum Mol Genet 2008;17:R23–R27.
8 Meissner A, Mikkelsen TS, Gu H et al. Genome-scale DNA methylation maps of pluripotent and differentiated cells. Nature 2008;454:766–770.
9 Kobayakawa S, Miike K, Nakao M et al. Dynamic changes in the epigenomic state and nuclear organization of differentiating mouse embryonic stem cells. Genes Cells 2007;12:447–460.
10 Mayer R, Brero A, von HJ et al. Common themes and cell type specific variations of higher order chromatin arrangements in the mouse. BMC Cell Biol 2005;6:44.
11 Meshorer E, Yellajoshula D, George E et al. Hyperdynamic plasticity of chromatin proteins in pluripotent embryonic stem cells. Dev Cell 2006;10:105–116.
12 Lin W, Dent SY. Functions of histone-modifying enzymes in development. Curr Opin Genet Dev 2006;16:137–142.
13 Efroni S, Duttagupta R, Cheng J et al. Global transcription in pluripotent embryonic stem cells. Cell Stem Cell 2008;2:437–447.
14 Gaspar-Maia A, Alajem A, Polesso F et al. Chd1 regulates open chromatin and pluripotency of embryonic stem cells. Nature 2009;460: 863–868.
15 Li E, Bestor TH, Jaenisch R. Targeted mutation of the DNA methyltransferase gene results in embryonic lethality. Cell 1992;69: 915–926.
16 Tsumura A, Hayakawa T, Kumaki Y et al. Maintenance of self-renewal ability of mouse embryonic stem cells in the absence of DNA methyltransferases Dnmt1, Dnmt3a and Dnmt3b. Genes Cells 2006; 11:805–814.
17 Lei H, Oh SP, Okano M et al. De novo DNA cytosine methyltransferase activities in mouse embryonic stem cells. Development 1996;122: 3195–3205.
18 Chen T, Ueda Y, Dodge JE et al. Establishment and maintenance of genomic methylation patterns in mouse embryonic stem cells by Dnmt3a and Dnmt3b. Mol Cell Biol 2003;23:5594–5605.
19 Jackson M, Krassowska A, Gilbert N et al. Severe global DNA hypomethylation blocks differentiation and induces histone hyperacetylation in embryonic stem cells. Mol Cell Biol 2004;24:8862–8871.
20 Chi AS, Bernstein BE. Developmental biology. Pluripotent chromatin state. Science 2009;323:220–221.

21 Szutorisz H, Georgiou A, Tora L et al. The proteasome restricts permissive transcription at tissue-specific gene loci in embryonic stem cells. Cell 2006;127:1375–1388.
22 van den Boom V, Kooistra SM, Boesjes M et al. UTF1 is a chromatin-associated protein involved in ES cell differentiation. J Cell Biol 2007;178:913–924.
23 Kooistra SM, Thummer RP, Eggen BJL. Characterization of human UTF1, a chromatin-associated protein with repressor activity expressed in pluripotent cells. Stem Cell Res 2009;2:211–218.
24 Zhao Y, Yin X, Qin H et al. Two supporting factors greatly improve the efficiency of human iPSC generation. Cell Stem Cell 2008;3:475–479.
25 Habara-Ohkubo A. Differentiation of beating cardiac muscle cells from a derivative of P19 embryonal carcinoma cells. Cell Struct Funct 1996;21:101–110.
26 O'Neill LP, Turner BM. Immunoprecipitation of native chromatin: NChIP. Methods 2003;31:76–82.
27 Martin-Magniette ML, Mary-Huard T et al. ChIPmix: mixture model of regressions for two-color ChIP-chip analysis. Bioinformatics 2008;24:i181–i186.
28 Johannes F, Wardenaar R, Colome-Tatche M et al. Comparing genome-wide chromatin profiles using ChIP-chip or ChIP-seq. Bioinformatics 2010;26:1000–1006.
29 Dempster AP, Laird LM, Rubin DB. Maximum likelihood from incomplete data via the EM algorithm. J R Stat Soc Ser B (Methodological) 1977;39:1–38.
30 Bolstad BM, Irizarry RA, Astrand M et al. A comparison of normalization methods for high density oligonucleotide array data based on variance and bias. Bioinformatics 2003;19:185–193.
31 Breitling R, Armengaud P, Amtmann A et al. Rank products: A simple, yet powerful, new method to detect differentially regulated genes in replicated microarray experiments. FEBS Lett 2004;573:83–92.
32 Livak KJ, Schmittgen TD. Analysis of relative gene expression data using real-time quantitative PCR and the 2(-Delta Delta C(T)) method. Methods 2001;25:402–408.
33 Shannon P, Markiel A, Ozier O et al. Cytoscape: A software environment for integrated models of biomolecular interaction networks. Genome Res 2003;13:2498–2504.
34 Maere S, Heymans K, Kuiper M. BiNGO: A Cytoscape plugin to assess overrepresentation of gene ontology categories in biological networks. Bioinformatics 2005;21:3448–3449.
35 Lehnertz B, Ueda Y, Derijck AA et al. Suv39h-mediated histone H3 lysine 9 methylation directs DNA methylation to major satellite repeats at pericentric heterochromatin. Curr Biol 2003;13:1192–1200.
36 Bailey TL, Williams N, Misleh C et al. MEME: Discovering and analyzing DNA and protein sequence motifs. Nucleic Acids Res 2006;34:W369–W373.
37 Marzluff WF, Duronio RJ. Histone mRNA expression: Multiple levels of cell cycle regulation and important developmental consequences. Curr Opin Cell Biol 2002;14:692–699.
38 Loh YH, Wu Q, Chew JL et al. The Oct4 and Nanog transcription network regulates pluripotency in mouse embryonic stem cells. Nat Genet 2006;38:431–440.
39 Ivanova N, Dobrin R, Lu R et al. Dissecting self-renewal in stem cells with RNA interference. Nature 2006;442:533–538.
40 Hu G, Kim J, Xu Q et al. A genome-wide RNAi screen identifies a new transcriptional module required for self-renewal. Genes Dev 2009;23:837–848.
41 Kim J, Chu J, Shen X et al. An extended transcriptional network for pluripotency of embryonic stem cells. Cell 2008;132:1049–1061.
42 Jiang J, Chan YS, Loh YH et al. A core Klf circuitry regulates self-renewal of embryonic stem cells. Nat Cell Biol 2008;10:353–360.
43 Yang J, Chai L, Fowles TC et al. Genome-wide analysis reveals Sall4 to be a major regulator of pluripotency in murine-embryonic stem cells. Proc Natl Acad Sci USA 2008;105:19756–19761.
44 Ogawa K, Nishinakamura R, Iwamatsu Y et al. Synergistic action of Wnt and LIF in maintaining pluripotency of mouse ES cells. Biochem Biophys Res Commun 2006;343:159–166.
45 Maison C, Almouzni G. HP1 and the dynamics of heterochromatin maintenance. Nat Rev Mol Cell Biol 2004;5:296–304.
46 Nishimoto M, Miyagi S, Yamagishi T et al. Oct-3/4 maintains the proliferative embryonic stem cell state via specific binding to a variant octamer sequence in the regulatory region of the UTF1 locus. Mol Cell Biol 2005;25:5084–5094.
47 Chuva de Sousa Lopes SM, van den DS, Carvalho RL et al. Altered primordial germ cell migration in the absence of transforming growth factor beta signaling via ALK5. Dev Biol 2005;284:194–203.
48 van Bragt MP, Roepers-Gajadien HL, Korver CM et al. Expression of the pluripotency marker UTF1 is restricted to a subpopulation of early A spermatogonia in rat testis. Reproduction 2008;136:33–40.
49 Zwaka TP. Keeping the noise down in ES cells. Cell 2006;127:1301–1302.
50 Dean W, Bowden L, Aitchison A et al. Altered imprinted gene methylation and expression in completely ES cell-derived mouse fetuses: Association with aberrant phenotypes Development 1998;125:2273–2282.
51 Humpherys D, Eggan K, Akutsu H et al. Epigenetic instability in ES cells and cloned mice. Science 2001;293:95–97.
52 Niwa H. Open conformation chromatin and pluripotency. Genes Dev 2007;21:2671–2676.


See www.StemCells.com for supporting information available online.